

EPR properties of $KY(WO_4)_2$ single crystals weakly doped with Er, Yb and Nd

H. Fuks^{a,*}, S.M. Kaczmarek^a, L. Macalik^b, J. Hanuza^b

^a Institute of Physics, Faculty of Mechanical Engineering and Mechatronics, West Pomeranian University of Technology in Szczecin, Poland

^b Institute of Low Temperature and Structure Research, PAS, P. Nr 1414, 50-950 Wrocław 2, Poland

ARTICLE INFO

Article history:

Available online 6 June 2012

Keywords:

EPR
Double tungstate
Er(III)
Yb(III)
Nd(III)

ABSTRACT

Well oriented $KY(WO_4)_2$ single crystal weakly doped simultaneously with Er, Yb and Nd have been investigated using EPR technique. Angular dependencies of the EPR lines clearly confirm C_2 symmetry of all: Er^{3+} , Yb^{3+} and Nd^{3+} dopants. Basic parameters of the spin Hamiltonian, including Zeeman and hyperfine terms (\mathbf{g} and \mathbf{A} matrices) as well the spatial orientation between principal axes system and crystallographic axes system were determined.

© 2012 Elsevier B.V. All rights reserved.

1. Introduction

Sensitized emission occurrence from the lanthanide ions (e.g., Er^{3+} , Yb^{3+}) has attracted significant attention and importance. It has been shown that the problems associated with finding a suitable pump band and with excited state absorption can be overcome in the erbium laser by co-doping with Yb [1,2]. The strong absorption band from $^2F_{7/2}$ to $^2F_{5/2}$ in Yb, which is centered on 950 nm, provides an ideal pump band for excitation of the $^4I_{11/2}$ level of Er.

For Yb^{3+} based lasers, various technical problems arise for high power operation; since the energy difference between excitation and emission is very small due to its two level configurations [3]. Good solution to overcome this difficulty is to sensitize it with Nd^{3+} ion. One can achieve an efficient lasing at 980 nm from Yb^{3+} on exciting the Nd^{3+} ion with easily available high power 800 nm laser diode [4,5].

Yb^{3+} ions can act as activators for Nd^{3+} and very efficient sensitizers for Er^{3+} , it can be expected to achieve improved energy transfer from Nd^{3+} to Er^{3+} in the presence of Yb^{3+} as bridging ions. In the paper [6], e.g., a fourfold emission enhancement at 1.54 μm of Er^{3+} ions has been achieved through an excitation of $^4F_{5/2}$ level of Nd^{3+} at 806 nm for the glass having 3 mol% Yb^{3+} with an energy transfer efficiency reaching up to 94%.

Co-doping of laser hosts with Er and Yb is important also in a case of infrared up-conversion materials, that can transfer infrared (IR) light to visible. Among them are fluorides, halides, sulfides due to low phonon energy and high luminous efficiency and also some oxides. We are interested in the families of double tungstates. They

are interesting materials due to phosphor and laser application but especially due to up-conversion effect. In the paper we analyze possibility of simultaneous doping of $KY(WO_4)_2$ single crystal with Er, Yb and Nd using EPR technique.

2. Experimental setup

Single crystals of the double potassium yttrium tungstate were grown by the thermal method developed by Borisov and Klevstova [7] and Klevtsov et al. [8]. For purpose of EPR measurements, intentional concentration of introduced RE^{3+} ions was assuming to be lower than 0.02 mol%. It was not verified experimentally. The cooling rate was 2 °C per hour and the obtained crystals were transparent and of good optical quality. The samples were checked for purity by the X-ray powder diffraction.

Raman spectra were measured using a Bruker RFS 100/S Raman Spectrometer with the back scattering configuration. The 1064 nm line of Nd:YAG laser was used as an excitation. Signal detection was performed with the LN-Ge (D418-T) liquid nitrogen-cooled NIR detector with an integrated preamplifier and high voltage power supply. The resolution of the Raman spectra was 2 cm^{-1} .

The electron paramagnetic resonance (EPR) spectra were recorded on a conventional X-band Bruker ELEXSYS E 500 CW-spectrometer operating at 9.5 GHz with 100 kHz magnetic field modulation in the temperature range 4–300 K. EPR–NMR program was applied to fit the EPR spectra. EPR measurements have been done at temperatures above 4 K with two crystal rotation modes, i.e. with magnetic field operating in ac - and ab -planes. It means that crystal was rotated around b - and c^* -crystallographic axes respectively, where c^* axis in monoclinic $KY(WO_4)_2$ system is chosen arbitrarily as being perpendicular to a - and b -crystallographic directions.

* Corresponding author.

E-mail address: fux@zut.edu.pl (H. Fuks).

3. Structure and Raman spectrum

The host crystal used in the present work crystallize in monoclinic space group $C2/c \equiv C_{2h}^6$ ($Z = 4$) [1]. In this structure the tungstate units built the WO_6 octahedra joined through the single and double oxygen bridges. The RE^{3+} ions occupy the sites of C_i and C_2 symmetry.

Raman spectrum of the $KY(WO_4)_2:Er, Nd, Yb$ single crystal including all vibrational modes is presented in Fig. 1. It consists of four strong bands in the $740\text{--}1000\text{ cm}^{-1}$ range (multiplets of the stretching $\nu(W\text{--}O)$ vibrations), two medium intensity bands in the $500\text{--}700\text{ cm}^{-1}$ range (stretching modes of the $W^O W$ and $W^O O W$ oxygen bonds), medium intensity bands in the $270\text{--}470\text{ cm}^{-1}$ range (banding vibrations) and group of medium bands in the $70\text{--}260\text{ cm}^{-1}$ range (translational motions of the cations and anions, as well as vibrations of the molybdate or tungstate polyhedra). The assignment to the respective normal modes presented in Fig. 1 was done according to the previous works [9–11]. As compare to double tungstates built of isolated tetrahedra, $KY(WO_4)_2$ polymeric crystal does not exhibit the gap between the 450 and 750 cm^{-1} region what means that there are some bands in this region confirmed the existence of the oxygen bridges.

Raman spectroscopy is not enough sensitive technique to analyze crystal structures with very low dopants concentration, so co-doping of our crystal with such small content of Er, Nd and Yb does not affect the spectra. That is one more reason why we decide to check the crystal content using EPR technique.

4. EPR results

Fig. 2a and b shows two examples of low temperature EPR spectra chosen in such a manner to have as much as possible details of the resonance lines visible. As could be seen, spectra consist of three narrow and intense lines with group of weaker satellite lines, emerging due to hyperfine interactions between electronic and nuclear magnetic moments. The number of hyperfine lines and their relative intensity enables to identify all three responsible paramagnetic centers as: Er^{3+} , Yb^{3+} and Nd^{3+} ions, where splitting of the lines is done by odd isotopes of rare earth ions. The presence of RE^{3+} ions in host $KY(WO_4)_2$ crystal is a consequence of natural contamination of basic metal oxides and has an important role, as far as optical properties of these materials.

All identified RE^{3+} ions are Kramer's type ions, where crystal field of $KY(WO_4)_2$ splits energy levels giving only the lowest doublet populated, with effective spin $S' = 1/2$. In this case the spin Hamiltonian could be described by the following equation:

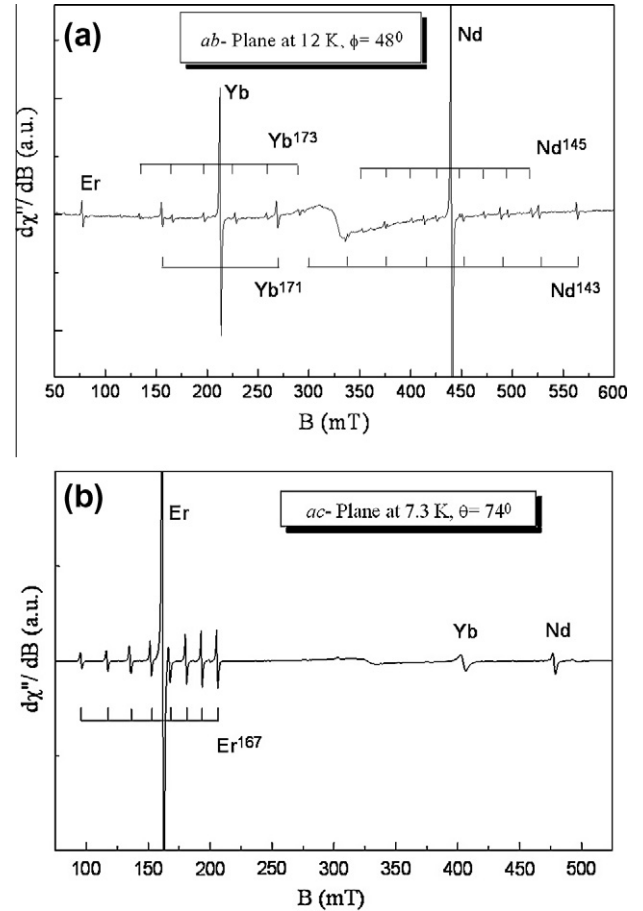


Fig. 2. Examples of the low temperature EPR spectra of $KY(WO_4)_2:Er, Nd, Yb$ crystal observed at magnetic field mode operation in: (a) ab -plane, (b) ac -plane.

$$H_s = \mu_B \mathbf{BgS}' + \mathbf{S}'\mathbf{AI}, \quad (1)$$

where the first term represents Zeeman interactions with an effective spin $S' = 1/2$ and the second one is responsible for the hyperfine interactions. The nuclear quadrupole term of odd RE^{3+} isotopes is neglected in this case as insignificant.

Fig. 3a and b shows angular dependencies (roadmaps) of the resonance lines observed while crystal was rotated around b - and c' -axes, i.e. magnetic field operated in ac - and ab -planes, respectively. For clarity, only the principal lines of even isotopes are shown on the patterns in Fig. 3. As could be seen, the angular dependence of Er^{3+} , Yb^{3+} and Nd^{3+} ions is fully resolved in both planes. All three paramagnetic centers revealed a low symmetry on their local crystallographic surrounding, suitable for a C_2 point symmetry.

According to well-known reports [12–15] RE^{3+} ions doped to $KY(WO_4)_2$ double tungstates are expected to occupy the yttrium crystallographic position with C_2 point symmetry in eightfold coordinated irregular polyhedra. The principal magnetic axes system of the RE^{3+} site generally do not coincides with crystallographic axes but, due to characteristic spatial orientation of RE^{3+} polyhedra, two magnetic axes: x and z are expect to lie in ac -plane, whereas third axis, defined as y , coincides with b -crystallographic direction.

Taking the above into account the analysis of the roadmap in ac -plane is very important. Extreme positions of the resonance lines determine the x - and z -magnetic axes, where, according to widely accepted definition, minimal value of magnetic resonance field indicates on the z direction. The general formula describing the low symmetry case has the form:

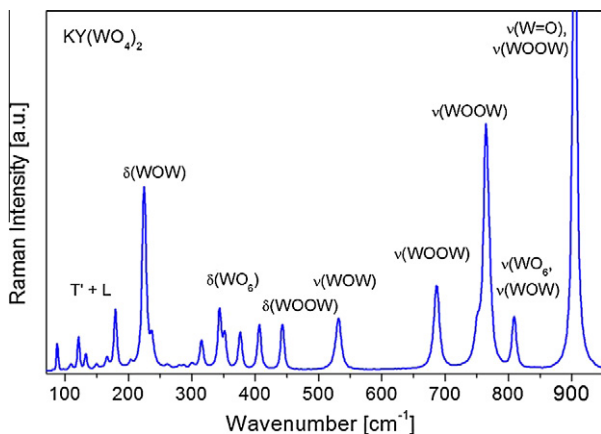


Fig. 1. Raman spectrum of low doped $KY(WO_4)_2:Er, Nd, Yb$ single crystal recorded at arbitrary direction.

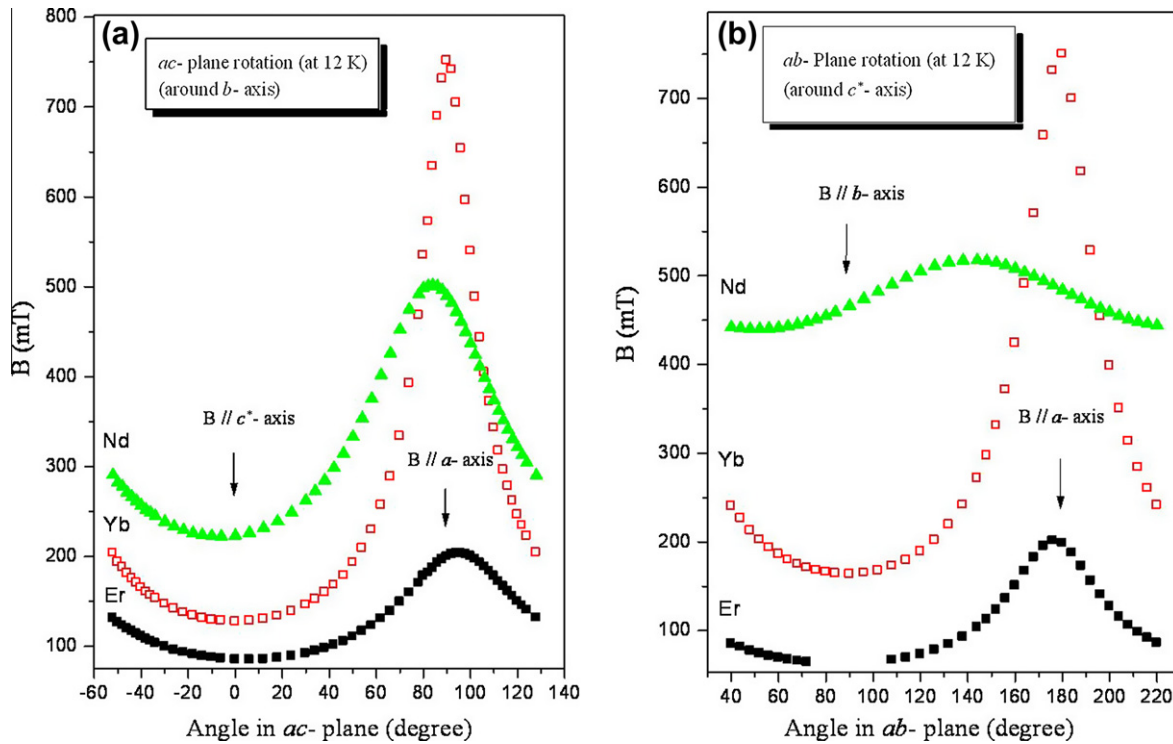


Fig. 3. The positions of the main resonance lines of the three RE³⁺ dopants in KY(WO₄)₂:Er, Nd, Yb crystal as a function of magnetic field direction. Angles represent polar and azimuthal angles of magnetic field in *abc*^{*}-axes system: (a) θ -relation, $\varphi = 0^\circ$, (b) φ -relation, $\theta = 90^\circ$.

$$g_{\text{eff}}^2 = g_z^2 \cos^2 \theta + g_x^2 \sin^2 \theta \cos^2 \varphi + g_y^2 \sin^2 \theta \sin^2 \varphi \quad (2)$$

In case of *ac*-operation plane, for *y* parallel to *b*, Eq. (2) is significantly reduced, as azimuthal angle φ is equal to zero.

In our estimation, see Fig. 3a, maximal and minimal position of the resonance lines are close to *a*- and *c*^{*}-axes, respectively. So,

estimated tilt, generally defined as a rotation angle between magnetic axes system (MAS) and crystallographic axes system (CAS), calculated between planes *ac*^{*}- and *xz*- seems to be very low, especially for Yb³⁺ ion. Detailed analysis of the EPR spectra in both rotation planes, including hyperfine lines of odd isotopes, has been done with employing the EPR–NMR procedure [16].

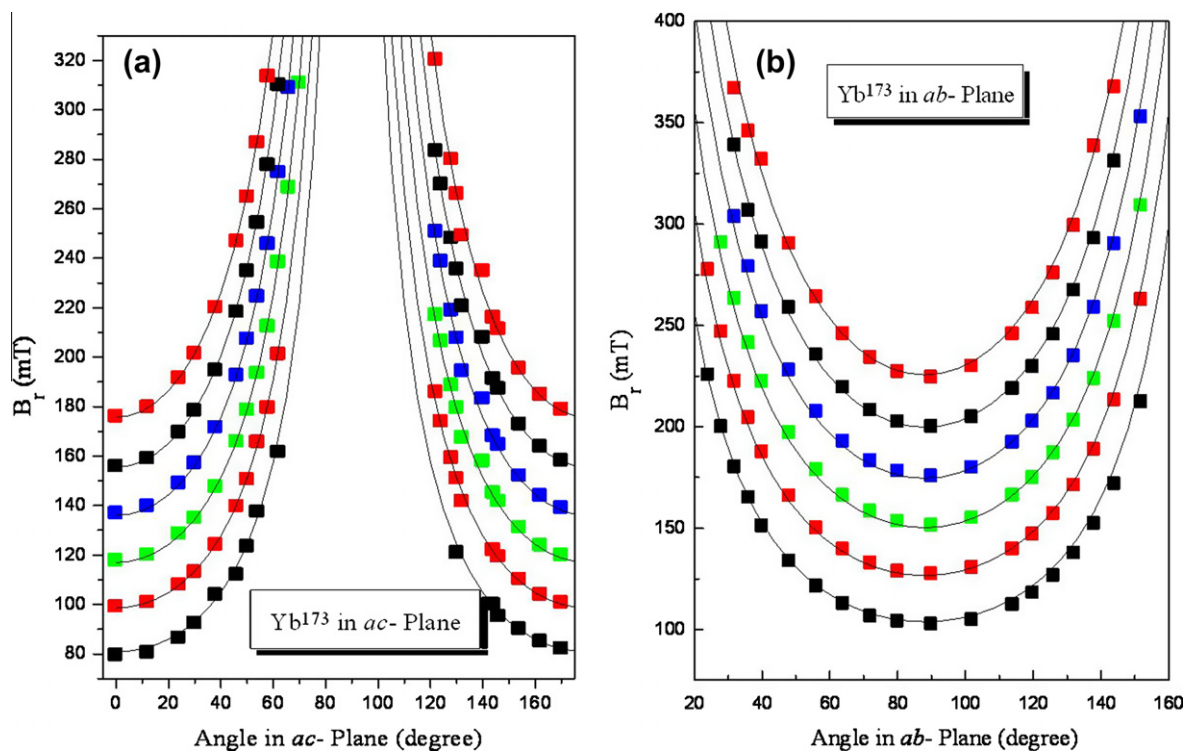


Fig. 4. Resonance positions of the six Yb¹⁷³ satellite lines (squares) and the fitting functions obtained by EPR–NMR simulation (solid lines) in (a) *ac* and (b) *ab* planes.

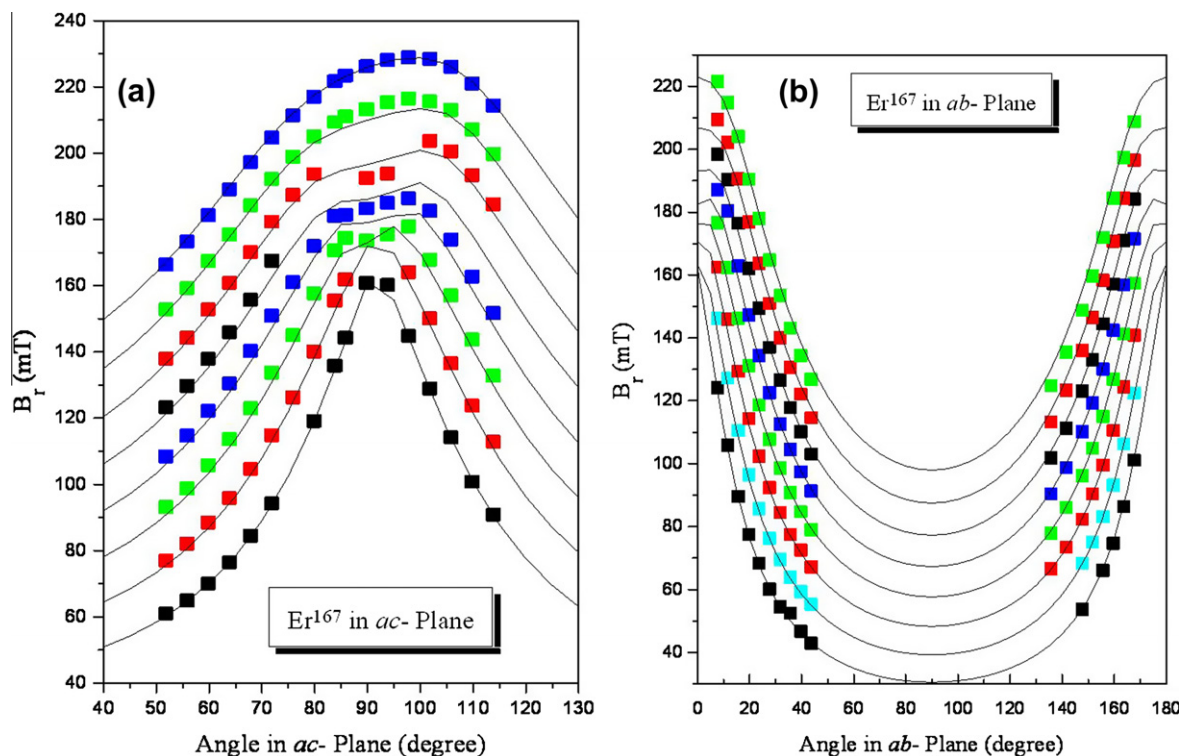


Fig. 5. The resonance positions of eight Er^{167} satellite lines (squares) and the fitting functions obtained by EPR-NMR simulation (solid lines) for (a) ac - and (b) ab -planes.

Fig. 4 a, b show results of the simulation performed for six hyperfine lines of Yb^{173} odd isotope ($I = 5/2$) observed in ac and ab planes, respectively. As could be seen, the result of simulation is enough good. Principal axes of \mathbf{g} and \mathbf{A} matrices coincide with crystallographic axes, i.e. no any significant tilt between xyz - and abc^* -systems was detected, including experimental errors. The principal values of \mathbf{g} and \mathbf{A} matrices for Yb^{173} odd isotope as well as the values for odd isotope Yb^{171} ($I = 1/2$) are collected in Table 1. The results for Yb^{171} isotope, that are not presented in Fig. 4, obtained by similar procedure, were to be very satisfying too.

Fig. 5a and b shows results of the EPR-NMR simulation made for eight hyperfine lines of Er^{167} isotope ($I = 7/2$) in two the same orthogonal planes of rotation. As could be seen, result of simulation is good enough. Principal axes of \mathbf{g} and \mathbf{A} matrices do not exactly coincide with abc^* -crystallographic system, what is visible as a slightly asymmetric shape of a pattern in ac -plane. As the pattern is symmetric in ab -plane it means that this plane contains C_2 crystallographic b -axis, simultaneously being coincident with y -direction of \mathbf{g} and \mathbf{A} matrices, as is expected for monoclinic symmetry (see for example [17]). According to results presented in Table 1 \mathbf{g} and \mathbf{A} matrices calculated for Er^{3+} indeed reveal coincidence of y -direction and a small tilt of xz -direction with respect to ac^* -system.

Fig. 6 shows an angular dependence of EPR lines for Nd^{143} isotope observed in ab -plane. Similar result in ac -plane is not presented here due to poor clarity, as the signal in this plane is weak or overlapped by other EPR lines. But analysis of the signal in ab -plane shows significant asymmetry of the pattern. It indicates that for neodymium ions discrepancy between xyz and abc^* -systems takes place not only in ac -plane, but additionally between y - and b -directions. The calculation of Nd^{even} isotopes in two different planes and $\text{Nd}^{143,145}$ isotopes in ac -plane enabled to evaluate the principal values of \mathbf{g} and \mathbf{A} matrices and their polar and azimuthal angles in respect to abc^* -system. Results presented in Table 1 confirm c.a. 4-degree tilt of g_y direction with respect to b -axis. Values of \mathbf{A} matrix were estimated for both $\text{Nd}^{143,145}$

Table 1

Principal values of \mathbf{g} and \mathbf{A} matrices for Yb^{3+} , Er^{3+} and Nd^{3+} odd isotopes. Errors of calculated values were less than 5%. θ and φ are polar and azimuthal angle coordinates of xyz -MAS axes system with respect to abc^* -CAS axes system. y -direction was established as a common direction for a set of principal axes of \mathbf{g} and \mathbf{A} matrices, other directions were chosen according to the following rule: x -value $<$ z -value.

| Ion | \mathbf{g} | θ | φ | \mathbf{A} (10^{-4} cm^{-1}) | θ | φ |
|-------------------|---------------|----------|-----------|--|----------|-----------|
| Yb^{173} | $g_x = 0.904$ | 90 | 0 | $A_x = 28$ | 90 | 0 |
| | $g_y = 4.126$ | 90 | 90 | $A_y = 324$ | 90 | 90 |
| | $g_z = 5.300$ | 0 | 0 | $A_z = 501$ | 0 | 0 |
| Yb^{171} | $g_x = 90$ | 90 | 0 | $A_x = 90$ | 90 | 0 |
| | $g_y = 800$ | 90 | 90 | $A_y = 800$ | 90 | 90 |
| | $g_z = 1810$ | 0 | 0 | $A_z = 1810$ | 0 | 0 |
| Er^{167} | $g_x = 3.326$ | 93 | 0 | $A_x = 125$ | 90.5 | 0 |
| | $g_y = 10.41$ | 90 | 90 | $A_y = 290$ | 90 | 90 |
| | $g_z = 7.944$ | 3 | 0 | $A_z = 500$ | 0.5 | 0 |
| Nd^{145} | $g_x = 0.862$ | 110 | -12 | $A_x = 170$ | | |
| | $g_y = 1.481$ | 94 | 80 | $A_y = 120$ | | |
| | $g_z = 3.303$ | 20 | 4 | $A_z = 370$ | | |
| Nd^{143} | $g_x = 106$ | | | $A_x = 106$ | | |
| | $g_y = 76$ | | | $A_y = 76$ | | |
| | $g_z = 236$ | | | $A_z = 236$ | | |

isotopes, but due to lack of data in ac -plane, coordinates of θ and φ are not presented in Table 1.

Spatial coincidence between xyz and abc^* systems for Yb^{3+} paramagnetic centers, calculated by us, is similar to those reported in Refs. [12,14], if one take into account something different crystallographic unit cell chosen by the authors. Principal values of \mathbf{g} matrix are comparable in the case of g_x and g_z values, whereas $g_y = 0.895$, reported in Ref. [12], is c.a. five times lower than ours, see Table 1.

For other above mentioned paramagnetic sites, inconsistency concerns tilt angles between xyz and abc^* systems. According to Ref. [13], if supposing Yb^{3+} centers as a base, tilt angle in ac plane should be c.a. 17° for Er^{3+} and c.a. 60° for Nd^{3+} . In our crystal, calculated angles are much lower, see Table 1.

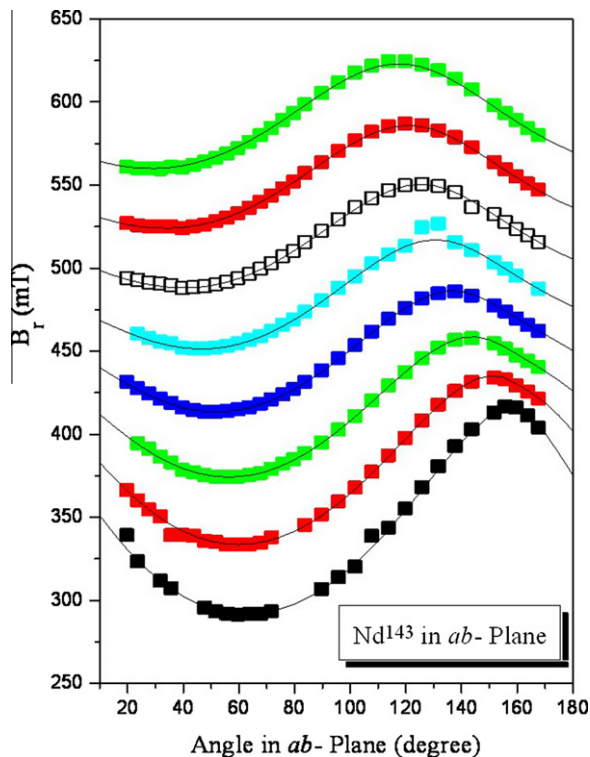


Fig. 6. Resonance position of eight Nd^{143} satellite lines (squares) and the fitting function obtained by EPR–NMR simulation in ab -plane (solid lines).

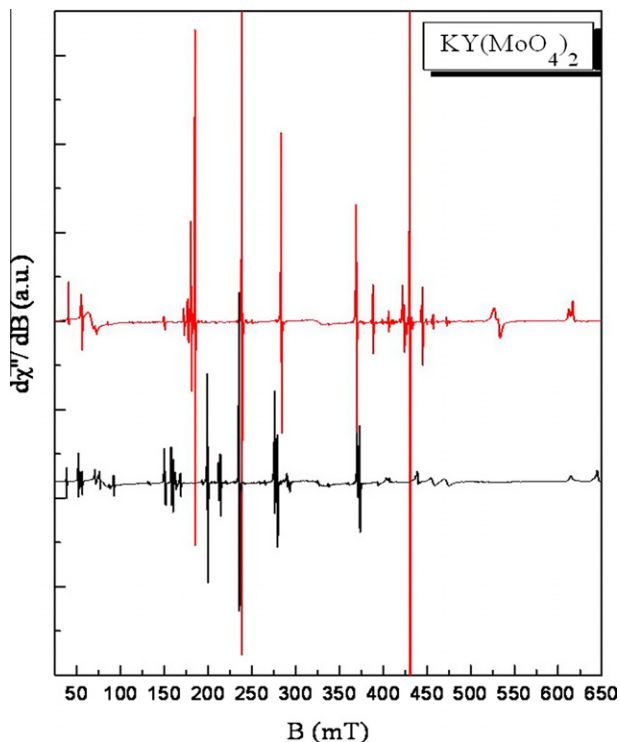


Fig. 7. EPR spectra of $\text{KY}(\text{MoO}_4)_2$ single crystal at temperature 8 K.

5. Conclusions

1. We confirmed C_2 symmetry of all three RE^{3+} ions, what means that these dopants occupy Y^{3+} position.

2. Having three different RE^{3+} ions in one crystal we were able to establish relatively spatial orientation between principal axes of Yb^{3+} , Er^{3+} and Nd^{3+} , independently on the possible experimental errors in fixing procedure.
3. We have established that principal axes of Yb and Er paramagnetic sites are tilted by c.a. 3° in ac -plane, whereas y axis is oriented along b crystal direction. For Nd ion we observed much bigger tilt in ac -plane and additional tilt between b - and y -axes with value of c.a. 4° .
4. The mismatch between abc^* and xyz systems could be attributed to increasing ionic radii of the above mentioned ions. Comparing values of ionic radii: $r = 112.5$ pm (Yb^{3+}), $r = 114.4$ pm (Er^{3+}) and $r = 124.9$ pm (Nd^{3+}) with ionic radius of host Y^{3+} ion having $r = 115.9$ pm, it is easy to see, that neodymium ion, having significantly bigger ionic radius, could deform C_2 polyhedra.
5. Principal values of \mathbf{g} and \mathbf{A} matrices and tilt angles, calculated by us, are not clearly comparable with those reported in Refs. [12–15]. One of the reason of such discrepancy may be extremely low ($\sim 0.02\%$) concentration of RE^{3+} dopants in the crystal investigated by us. Because we have not observed EPR signals from Yb^{3+} pairs the reason of the discrepancy should be verified in the next future.

In this paper we presented a detailed description of the three RE^{3+} dopants, Yb, Er and Nd, in nominally nonmagnetic $\text{KY}(\text{WO}_4)_2$ single crystal, that existed in our crystal as a residual contamination of Y_2O_3 basic oxide, with very low concentration. The existence of the RE^{3+} dopants enables to control optical properties of double tungstates. Similar coexistence of the RE^{3+} ions we observed previously in other, potentially nonmagnetic $\text{KY}(\text{MoO}_4)_2$ single crystal. In paper [18] we reported a strong complex signal built of narrow and intense EPR lines (Fig. 7). In the view of present results, the group of lines observed in the EPR spectra of $\text{KY}(\text{MoO}_4)_2$ crystal could arise from the small quantity of different RE^{3+} ions, with possible complex dipolar and exchange interactions.

References

- [1] D.C. Hanna, A. Kazer, D.P. Shepherd, *Opt. Commun.* 63 (1987) 417.
- [2] M.E. Fermann, D.C. Hanna, D.P. Shepherd, P.J. Suni, J.E. Townsend, *Electron. Lett.* 24 (1988) 1135.
- [3] E.H. Jonas, J. Björn, P. Valdas, L. Fredrik, *Opt. Express* 15 (2007) 13930–13935.
- [4] B.L. Davidov, A.A. Krylov, *Quantum Electron* 37 (2007) 843–846.
- [5] F. Liegard, J.L. Doualan, R. Moncorge, M. Bettinelli, *Appl. Phys. B* 80 (2005) 985–991.
- [6] D.A. Sontakke, B. Kaushik, K.M. Ashis, A. Kalyandurg, *J. Fluoresc.* 20 (2010) 425–434.
- [7] S.V. Borisov, R.F. Klevtsova, *Kristallografiya* 13 (1968) 517.
- [8] P.V. Klevtsov, L.P. Kozeeva, L.Yu. Kharchenko, *Kristallografiya* 20 (1975) 1210.
- [9] L. Macalik, J. Hanuza, B. Macalik, W. Ryba-Romanowski, S. Gołab, A. Pietraszko, *J. Lumin.* 79 (1998) 9.
- [10] L. Macalik, J. Hanuza, A.A. Kaminskii, *J. Molec. Struct.* 555 (2000) 289.
- [11] L. Macalik, J. Hanuza, A.A. Kaminskii, *J. Raman Spectrosc.* 33 (2002) 92.
- [12] A.D. Prokhorov, M.T. Borowiec, M.C. Pujol, I.M. Krygin, A.A. Prokhorov, V.P. Dyakonov, P. Aleshkevych, T. Zayarnyuk, H. Szymczak, *Eur. Phys. J. B* 55 (2007) 389–395.
- [13] A.D. Prokhorov, M.T. Borowiec, V.P. Dyakonov, V.I. Kamenev, A.A. Prokhorov, P. Aleshkevych, T. Zayarnyuk, H. Szymczak, *Physica B* 403 (2008) 3174–3178.
- [14] M.C. Pujol, M. Aguilo, F. Diaz, M.T. Borowiec, A.D. Prokhorov, V.P. Dyakonov, A. Nabialek, S. Piechota, H. Szymczak, *Physica B* 388 (2007) 257–260.
- [15] M.T. Borowiec, A.A. Prokhorov, A.D. Prokhorov, V.P. Dyakonov, H. Szymczak, *J. Phys. Condens. Matter* 15 (2003) 5113–5119.
- [16] M.J. Mombourquette, J.A. Weil, D.G. McGavin, *EPR–NMR User's Manual*, Department of Chemistry, University of Saskatchewan, Saskatoon, SK, Canada, 1999.
- [17] T.H. Yeom, C. Rudowicz, S.H. Choh, D.G. McGavin, *Phys. Stat. Sol. (b)* 198 (1996) 839.
- [18] H. Fuks, S.M. Kaczmarek, G. Leniec, L. Macalik, B. Macalik, J. Hanuza, *Opt. Mat.* 32 (2010) 1560–1567.